



Virginia Commonwealth University
VCU Scholars Compass

Electrical and Computer Engineering Publications

Dept. of Electrical and Computer Engineering

2003

Contactless electroreflectance, in the range of 20 K $< T < 300$ K, of freestanding wurtzite GaN prepared by hydride-vapor-phase epitaxy

Y. S. Huang

Brooklyn College of the City University of New York

Fred H. Pollak

Brooklyn College of the City University of New York

S. S. Park

Samsung Advanced Institute of Technology

K. Y. Lee

Samsung Advanced Institute of Technology

H. Morkoç

Virginia Commonwealth University

Follow this and additional works at: http://scholarscompass.vcu.edu/egre_pubs

 Part of the [Electrical and Computer Engineering Commons](#)

Huang, Y. S., Pollak, F. H., Park, S. S., et al. Contactless electroreflectance, in the range of 20 K

Downloaded from

http://scholarscompass.vcu.edu/egre_pubs/181

This Article is brought to you for free and open access by the Dept. of Electrical and Computer Engineering at VCU Scholars Compass. It has been accepted for inclusion in Electrical and Computer Engineering Publications by an authorized administrator of VCU Scholars Compass. For more information, please contact libcompass@vcu.edu.

Contactless electroreflectance, in the range of $20\text{ K} < T < 300\text{ K}$, of freestanding wurtzite GaN prepared by hydride-vapor-phase epitaxy

Y. S. Huang^{a)} and Fred H. Pollak^{b)}

Physics Department and New York State Center for Advanced Technology in Ultrafast Photonic Materials and Applications, Brooklyn College of the City University of New York, Brooklyn, New York 11210-2889

S. S. Park and K. Y. Lee

Samsung Advanced Institute of Technology, P.O. Box 111, Suwon, Korea 440-600

H. Morkoç

Department of Electrical Engineering and Physics Department, Virginia Commonwealth University, Richmond, Virginia 23284-3072

(Received 2 July 2002; accepted 22 April 2003)

We have performed a detailed contactless electroreflectance study of the interband excitonic transitions on both the Ga and N faces of a 200- μm -thick freestanding hydride-vapor-phase-epitaxy grown wurtzite GaN sample with low defect concentration in the temperature range between 20 and 300 K. The transition energies of the A, B, and C excitons and broadening parameters of the A and B excitons have been determined by least-square fits to the first derivative of a Lorentzian line shape. The energy positions and separations of the excitonic transitions in the sample reveal the existence of residual strain. At 20 K the broadening parameter of A exciton deduced for the Ga (5×10^5 dislocation cm^{-2}) and N (1×10^7 dislocation cm^{-2}) faces are 3 and 7 meV, respectively, indicating a lower defect concentration on the former face. The parameters that describe the temperature dependence of the interband transition energies of the A, B, and C excitons as well as the broadening function of the A and B features are evaluated. The results from an analysis of the temperature dependence of the broadening function of excitons A and B indicate that GaN exhibits a very large exciton-phonon coupling. © 2003 American Institute of Physics.
[DOI: 10.1063/1.1582230]

I. INTRODUCTION

Epitaxial GaN and its alloys with Al and In are emerging wide-gap semiconductors well suited to fabrication of semiconductor devices including visible-ultraviolet light emitting diodes, visible-ultraviolet detectors, and high temperature, high frequency transistors.¹⁻⁴ Much improved device performance could be facilitated by the development of high-quality freestanding GaN substrates with tailored electrical properties. One rapidly advancing source of thick, freestanding GaN wafers is hydride-vapor-phase epitaxy (HVPE),⁵ which is a promising candidate for this substrate role. There have been numerous studies reporting the evidence of fine structures observed in the energy region near the band edge of GaN using various optical measurements.⁶⁻¹² In spite of these detailed studies, there have been some discrepancies in the description of the excitonic transition energies and their temperature dependence in GaN. Previously we have studied the temperature dependence of the energies and linewidths of the A, B, and C excitons associated with the direct gap of wurtzite GaN (WZ-GaN)/sapphire (0001) by using the con-

tactless electroreflectance (CER) technique.¹³ The results show that as the temperature increases the separation between the A, B, and C excitonic energies becomes larger and the possible origin of this effect was attributed to the difference in the thermal expansion coefficients between the GaN and the sapphire substrate, which generates some compressive stress. In order to verify this interpretation we have performed a similar study on a high quality freestanding WZ-GaN sample.

In this article we report a detailed investigation of the temperature dependence of the CER measurements on both the Ga and N faces of a freestanding HVPE-grown WZ-GaN sample with low defect concentration in the temperature range between 20 and 300 K. The energies and broadening parameters of the relevant excitonic transitions are evaluated by least-square fits to the first derivative of a Lorentzian line shape. The temperature dependence of the interband excitonic transition energies has been fit by both Varshni¹⁴ and Bose-Einstein-type¹⁵ equations. The temperature variation of the broadening function of the A and B features has also been studied in terms of a Bose-Einstein-type expression that contains the exciton-longitudinal optical (LO) ($q \approx 0$) phonon coupling constant.¹⁶

II. EXPERIMENT

The sample was grown by HVPE on a (0001) sapphire substrate to a thickness of $\sim 300\ \mu\text{m}$. In order to obtain a

^{a)}Permanent address: Department of Electronic Engineering, National Taiwan University of Science and Technology, Taipei, Taiwan 106, Republic of China.

^{b)}Author to whom correspondence should be addressed. Also at Graduate School and University Center of the City University of New York, New York, NY 10016; electronic mail: fpollak@brooklyn.cuny.edu

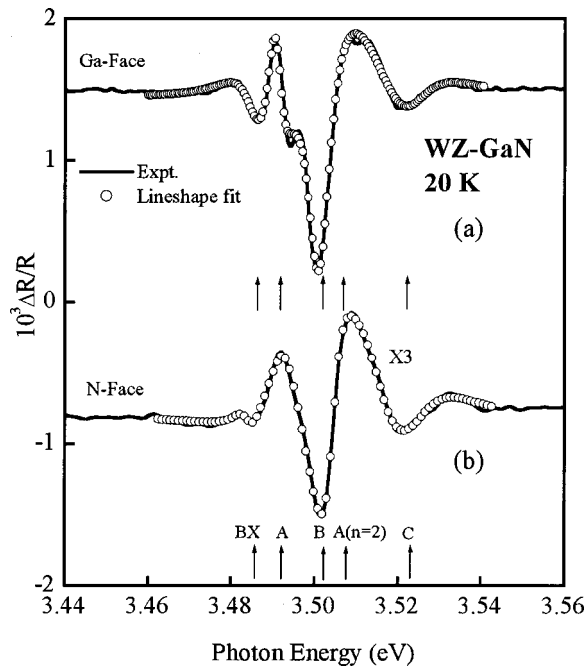


FIG. 1. The solid lines are the CER spectra of the (a) Ga and (b) N face of a freestanding WZ-GaN sample at 20 K. The dotted curves are least-square fits to Eq. (1). The identifications of the various spectral features are given by the notations BX (bound exciton), A, B, A($n=2$), and C excitonic transitions with the vertical arrows.

freestanding sample, the thick GaN layer was separated from the sapphire by laser-induced lift-off.¹⁷ The GaN wafer was then mechanically polished and dry etched down to a final thickness of $\sim 200 \mu\text{m}$. Both the Ga and N faces were independently etched in hot phosphoric acid (H_3PO_4) to reveal the defects as examined by atomic force microscopy imaging. The Ga and N faces of the c -plane GaN exhibited defect concentrations of 5×10^5 and $1 \times 10^7 \text{ cm}^{-2}$, respectively.¹⁸

The CER method utilizes a condenser-like system consisting of a front wire grid with a second copper electrode separated from the first electrode by insulating spacers.¹⁹ The sample is placed between these two capacitor plates. The dimensions of the spacer are such that there is a very thin layer ($\sim 0.1 \text{ mm}$) of air (or vacuum) between the front surface of the sample and the wire grid of the first electrode. Thus, there is nothing in direct contact with the front surface of the sample. The ac modulating voltage ($\sim 1 \text{ kV}$ peak to peak at $\sim 200 \text{ Hz}$) is applied between the copper strip and the front wire grid electrode. The CER method has a number of advantages over photoreflectance (PR) for the study of wide-band-gap nitride materials. It does not require an UV laser as the pump beam and it also avoids the photoluminescence background due to the pump beam.

III. RESULTS AND DISCUSSION

The solid curves in Figs. 1(a) and 1(b) are the experimental CER spectra at 20 K for the Ga and N faces, respectively, of the freestanding WZ-GaN sample. The curves have been displaced for clarity. The dotted curves are least-square fits to the first derivative of a Lorentzian line shape functional form¹⁹

$$\frac{\Delta R}{R} = \text{Re} \left[\sum_j^p C_j e^{i\theta_j} (E - E_j + i\Gamma_j)^{-2} \right], \quad (1)$$

where p is the number of spectral features to be fitted, E is the photon energy, C_j , θ_j , E_j , and Γ_j are the amplitude, phase, energy, and broadening parameter of the j th feature, respectively. This form is appropriate for bound states such as excitons and impurities. The CER spectra exhibit three prominent structures corresponding to intrinsic free-exciton transitions labeled by A, B, and C with the vertical arrows. These excitons are related to the $\Gamma_9^V - \Gamma_7^C$, Γ_7^V (upper band)- Γ_7^C and Γ_7^V (lower band)- Γ_7^C interband transitions, respectively. The energy positions for the A, B, and C exciton transitions on both the Ga and N faces are 3.491 ± 0.001 , 3.501 ± 0.001 , and $3.522 \pm 0.001 \text{ eV}$, respectively. Reynolds *et al.*²⁰ reported 3.4903, 3.4997, and 3.5271 eV, respectively, in GaN grown on sapphire by molecular beam epitaxy. These numbers are somewhat higher than the values obtained from virtually strain-free GaN layers,^{9,10} but similar to those obtained from the GaN thin films grown on sapphire substrates.^{8,11} Shan *et al.*¹¹ reported a reflectance and photoreflectance (PR) study on undoped GaN thin films grown by metalorganic-chemical-vapor deposition on (0001) sapphire substrates at 10 K. The energy positions for the A, B, and C excitonic transitions were determined to be 3.491, 3.499, and 3.528 eV, respectively. The differences between these films and the strain-free bulk films were attributed to the effects of residual strain caused by the mismatch of lattice parameters and thermal expansion coefficients between the GaN epilayer and the substrate. The results of our study show that $E_{A,B} - E_{A,B}^{\text{strain-free}} \approx 10 \text{ meV}$ and $\Delta E_{A,C} - \Delta E_{A,C}^{\text{strain-free}} \approx 10 \text{ meV}$, which indicates a residual in-plane compressive strain of about 0.03%.²¹

We have also observed that at 20 K the linewidth of the N face is much broader than that of Ga face, i.e., about 7 and 3 meV, respectively. This result indicates a lower defect concentration on the Ga face in relation to the N surface, in agreement with the atomic force microscopy study of 5×10^5 and $1 \times 10^7 \text{ dislocations cm}^{-2}$, respectively.¹⁸ Recently Chichibu *et al.*²² reported an optical study on GaN films grown toward the Ga and N faces. The GaN film grown toward the Ga face exhibited clear excitonic features in its optical absorption and luminescence spectra up to room temperature, while the film grown toward the N face exhibited a broad emission band, located in a broad absorption tail. The difference between the two was explained in terms of the presence of impurity-induced band-tail states in the N face of GaN due to increased impurity density and incorporation of large volume vacancy-type defects.

A small feature [denoted as BX (bound exciton)] located at an energy $\sim 6 \text{ meV}$ below the A exciton is attributed to an exciton bound to a neutral shallow donor transition. Similar results were reported by Chichibu *et al.*⁷ for the GaN films on sapphire (0001) substrates. Furthermore, in order to obtain a better fit of the spectrum, an additional feature needed to be included at $\sim 16 \text{ meV}$ above feature A. This structure can be identified with the $n=2$ excited state ($2s$) of the A exciton.⁷ Such identification permits a direct estimate of the binding energy for the A exciton from the separation between

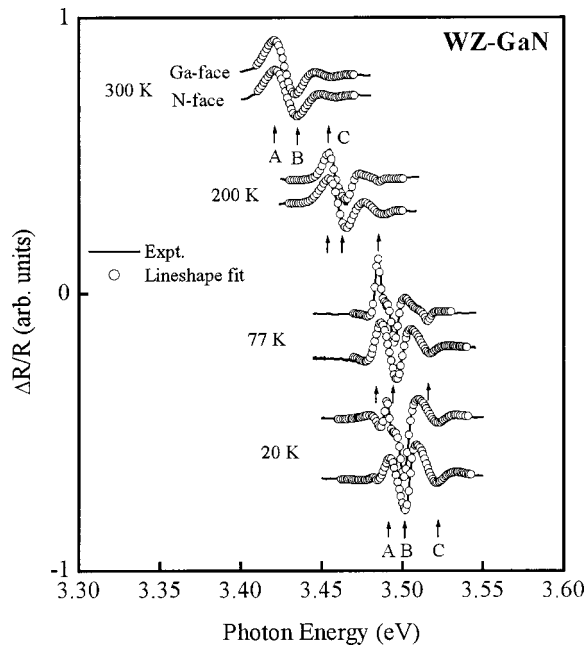


FIG. 2. The solid curves are the experimental CER spectra of the Ga and N faces of a freestanding WZ-GaN film. The Ga-face spectra are a factor of 3 larger than the N-face signals. The dotted curves are least-square fits to the first derivative of a Lorentzian profile. For clarity the curves are displaced and only the obtained A, B, and C exciton energies are shown by arrows.

the $n=1$ and $n=2$ states assuming the hydrogenic model based on the effective mass approximation is applicable. According to Elliott's theory,²³ exciton energy levels are given as

$$E_n^{\text{exc}} = -\frac{E_b^{\text{exc}}}{n^2}, \quad (2)$$

where n is an integer and E_b is the binding energy. From the results presented above, we obtain a binding energy of $E_b \sim 21$ meV. Ground and excited states of excitons in a photoluminescence/PR experiment,²⁰ were previously utilized to determine the binding energy for the A and B excitons to be 21 meV while 23 meV was found for the C exciton, which is excellent agreement with our results. In addition, the present value agrees well with a previous report on the binding energy for the intrinsic excitons in GaN by Shan *et al.*¹¹

In Fig. 2 the solid lines represent the experimental CER spectra of the Ga (N) face of the freestanding GaN film at 20, 77, 200, and 300 K, respectively. For clarity the curves are displaced. As in Fig. 1 the signals from the Ga face are about a factor of 3 larger than those from the N surface. As the temperature increases, the CER spectral features redshift and broaden. The dotted curves are least-square fits to the first derivative of a Lorentzian profile,¹⁹ which yields the interband excitonic transition energies. At low temperatures the transition of the first excited state of the A exciton is included. For clarity only the obtained A, B, and C exciton energies are shown by arrows in Fig. 2.

Based on electromodulation theory which takes into account both ac modulating and dc fields,¹⁹ the fact that the signal from the Ga face is about three times larger in relation

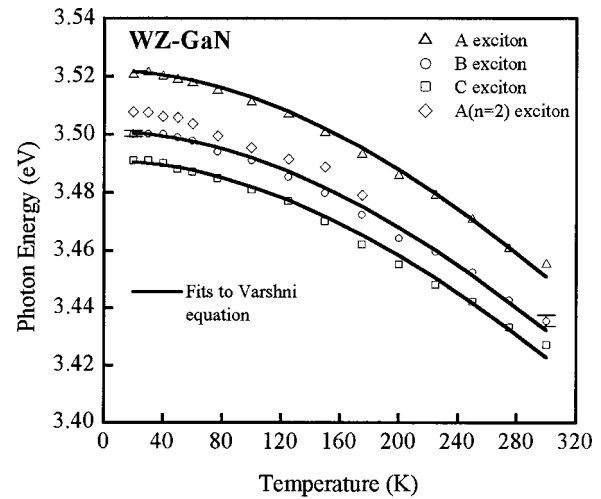


FIG. 3. The transition energies of the A, B, A ($n=2$), and C excitons obtained from the CER spectra of a freestanding WZ-GaN sample as a function of temperature. The solid lines are least-square fits to the Varshni equation.

to the N surface indicates that the built-in field on the former is about a factor of 1.4 larger than that of the latter. In addition, the phase of the signals from both surfaces indicates an n -type band bending.²⁴

Plotted in Fig. 3 are the experimental values of the transition energies $E_A(T)$, $E_B(T)$, and $E_C(T)$ corresponding to the A, B, and C excitons, respectively, as well as the first excited state of the A exciton (for temperatures lower than 200 K). Representative error bars are shown. In contrast with our previous observations for WZ-GaN¹³ and WZ-Al_{0.05}Ga_{0.95}N²⁵ films on sapphire substrates, the splitting between the A, B, and C excitonic transition energies remains unchanged, within experimental error, in the temperature range between 20 and 300 K. This indicates that for a freestanding sample the A, B, and C excitons have essentially the same temperature dependence. The result confirms our previous reports^{13,25} that as the temperature increases the difference in the thermal expansion coefficients between the GaN (AlGaN) and the sapphire substrate generates some in-plane compressive stress, causing the splitting between the A, B and C excitonic energies to become larger.

The solid curves in Fig. 3 are least-square fits to the Varshni empirical relationship¹⁴

$$E(T) = E(0) - \alpha T^2 / (\beta + T), \quad (3)$$

where $E(0)$ is the excitonic transition energy at 0 K, and α and β are the Varshni coefficients. The obtained values of $E(0)$, α , and β for the three interband excitonic transitions of the freestanding WZ-GaN sample are listed in Table I. For comparison purposes, we have also listed numbers for some representative previous reports of WZ-GaN.^{6,13} More complete values of related material can be found in Ref. 21. The numbers for α and β are in good agreement with our previous values for the A and B transitions determined from CER measurements on a GaN/sapphire (0001) sample.¹³

The temperature dependence of the interband transition energies also can be described by a Bose-Einstein-type expression¹⁵

TABLE I. Values of the Varshni- and Bose-Einstein-type fitting parameters which describe the temperature dependencies of the A, B, and C excitons in WZ-GaN.

Material	$E(0)$ (eV)	α (10^{-4} eV/K)	β (K)	a_B (meV)	Θ_B (K)
GaN ^{a,b}					
A exciton	3.490 ± 0.001	10.4 ± 0.8	1100 ± 100	75 ± 20	350 ± 50
B exciton	3.500 ± 0.001	10.5 ± 0.8	1100 ± 100	75 ± 20	350 ± 50
C exciton	3.520 ± 0.001	10.6 ± 0.8	1100 ± 100	76 ± 20	350 ± 50
GaN ^{c,d}					
A exciton	3.484 ± 0.002	12.8 ± 2.0	1190 ± 150	110 ± 20	450 ± 100
B exciton	3.490 ± 0.002	12.9 ± 2.0	1280 ± 150	112 ± 20	420 ± 100
C exciton	3.512 ± 0.004	6.6 ± 3.0	840 ± 300	57 ± 30	340 ± 100
GaN ^{d,e}	3.492	11.8	1414		
GaN ^{f,g}	3.480			81	366

^aPresent work (contactless electroreflectance).

^bFree-standing WZ-GaN sample prepared by HVPE.

^cReference 13 (contactless electroreflectance).

^dWZ-GaN/sapphire (0001).

^eReference 6 (absorption).

^fReference 7 (photoreflectance).

^gFree-standing WZ-GaN sample prepared by lateral epitaxial overgrowth.

$$E(T) = E(0) - 2a_B / [\exp(\Theta_B/T) - 1], \quad (4)$$

where $E(0)$ is the transition energy at 0 K, a_B represents the strength of the exciton-average phonon (optical and acoustical) interaction, and Θ_B corresponds to the average phonon temperature. The temperature dependence of the A, B, and C features has been fit to Eq. (4) and the obtained values of the relevant parameters also are given in Table I. For comparison purposes, also presented in Table I are some other representative results for WZ-GaN.^{7,13} More complete values of these quantities for related materials can also be found in Ref. 21. The obtained parameters are in a reasonable agreement with our previous values obtained from WZ-GaN/sapphire (0001)¹³ and the values determined from PR measurements on a nearly freestanding GaN substrate prepared by lateral epitaxial overgrowth.⁷

The temperature shift of interband transition energies is mainly due to the interactions of the exciton with relevant acoustic and optical phonons. According to the existing theory²⁶ this lead to a value of Θ_B significantly smaller than the LO-phonon ($q \approx 0$) temperature. Our result of $\Theta_B = 350$ K, which is much smaller than the LO-phonon temperature $\Theta_{LO} = 1064$ K for GaN,⁶ is in agreement with this theoretical consideration.

The experimental values of the temperature dependence of the linewidth $\Gamma(T)$ of the A and B excitons for the Ga (N) face, as obtained from the line shape fit, are displayed by the open triangles and squares in Fig. 4, respectively. Representative error bars are shown. Initially, $\Gamma(T)$ increases linearly with T , but begins to be superlinear starting from about 150 K. The temperature dependence of the linewidth of excitonic transition of semiconductors can be expressed as¹⁶

$$\Gamma(T) = \Gamma(0) + \gamma_{AC}T + \Gamma_{LO} / [\exp(E_{LO}/kT) - 1], \quad (5)$$

where $\Gamma(0)$ represent the broadening invoked from temperature-independent mechanisms, such as impurities, point and extended defects, surface scattering, and electron-electron interactions, whereas the second term corresponds to

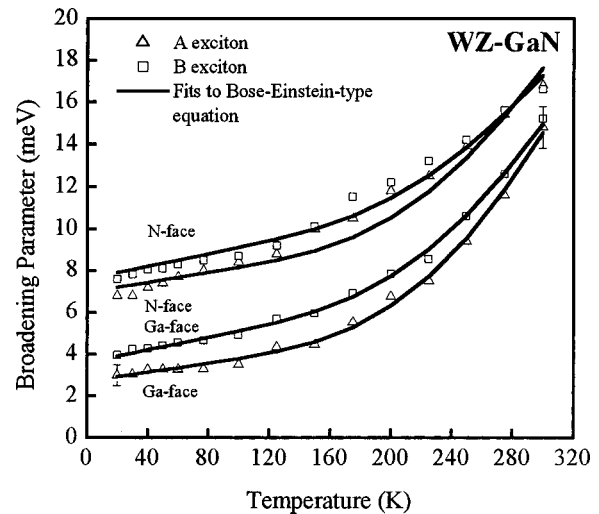


FIG. 4. The experimental temperature-dependent linewidth $\Gamma(T)$ of the A and B exciton features for the Ga and N faces of a freestanding WZ-GaN sample. The solid lines are least-square fits to Eq. (5) with $E_{LO} = 91.7$ meV and $\gamma_{AC} = 15 \mu\text{eV/K}$.

lifetime broadening due to the exciton-acoustical phonon interaction, where γ_{AC} is the acoustical phonon coupling constant. The third term is caused by the exciton-LO phonon ($q \approx 0$) (Fröhlich) interaction. The quantity Γ_{LO} represents the strength of the exciton-LO phonon coupling while E_{LO} is the LO phonon energy and k is Boltzmann's constant. Because of the error bars on our data it was necessary to fix the parameters γ_{AC} and E_{LO} in order to obtain the two significant quantities of $\Gamma(0)$ and Γ_{LO} by means of a least-square fit, where the values of $\gamma_{AC} = 15 \mu\text{eV/K}$ and $E_{LO} = 91.7$ meV were used as adopted from a previous report by Fischer *et al.*⁶

The solid lines in Fig. 4 are least-square fits to Eq. (4), which made it possible to evaluate $\Gamma(0)$ and Γ_{LO} for the Ga and N faces of GaN, respectively. The obtained values are listed in Table II. For comparison we also have displayed in Table II values of Γ_{LO} in terms of full width at half maximum for GaN,^{6,13,27,28} Ga_{0.95}Al_{0.05}N,²⁵ GaAs,²⁹ and ZnSe³⁰ from other works. It should be noticed that some of the previous investigations of $\Gamma(T)$ have neglected the acoustical phonon term in the interpretation of the data. The values of $\Gamma(0)$ and Γ_{LO} for the A feature determined are 3.0 ± 0.5 (7.0 ± 0.5) meV and 250 ± 20 (200 ± 20) meV, respectively, for Ga (N) face. The smaller value of $\Gamma(0)$ for the Ga face reveals a better quality (lower defect concentration) of the material. Compared to the values for GaAs (23 ± 1.5 meV)²⁹ and ZnSe (24 ± 8 meV),³⁰ the exciton-LO phonon coupling parameter obtained by the fit to Eq. (5) is extremely large. Other recent linewidth analyses of excitons in GaN performed using other experimental techniques also report large exciton-phonon interaction.^{6,13,27,28} The much larger value of Γ_{LO} for GaN might be due to the much larger E_{LO} of GaN (~ 92 meV)⁶ in comparison to that of ZnSe (31 meV).³⁰ In addition, it is possible that a larger deformation potential interaction, which may account for a significant fraction of Γ_{LO} in addition to the Fröhlich interaction, is responsible for the larger Γ_{LO} .

TABLE II. Values of the parameters that describe the temperature dependence of Γ (in terms of half width half maximum) of the A and B exciton features for the Ga and N faces of the freestanding WZ–GaN sample. For comparison purposes the phonon coupling parameters for the excitonic transitions of other WZ–GaN, WZ–Ga_{0.95}Al_{0.05}N, GaAs, and ZnSe from previous works also are listed.

Material	$\Gamma_o(0)$ (meV)	Γ_{LO} (meV)	E_{LO} (meV)	γ_{AC} ($\mu\text{eV/K}$)
GaN ^{a,b}				
Ga face				
A exciton	3.0±0.5	250±20	91.7 ^c	15 ^c
B exciton	4.0±0.5	230±20	91.7 ^c	15 ^c
N face				
A exciton	7.0±0.5	200±20	91.7 ^c	15 ^c
B exciton	7.5±0.5	170±20	91.7 ^c	15 ^c
GaN ^{d,e}	10	375	91.7 ^c	15
GaN ^{e,f}	2.4	390	91.7 ^c	16
GaN ^{e,g}				
A exciton	15±2	60±20	63±8.6	
B exciton	13±2	74±20	66.6±8.6	
GaN ^{e,h}	34.5	104	68.9 ^c	
Ga _{0.95} Al _{0.05} N ⁱ				
A exciton	12±2	91±20	63.4±8.6	
B exciton	11±2	122±20	67.1±8.6	
GaAs ^j	2	23±1.5	35.9 ^c	
ZnSe ^k	6.5±2.5	24±8	31	2.0

^aPresent work (contactless electroreflectance).

^bFree-standing WZ–GaN sample prepared by HVPE.

^cParameter fixed.

^dReference 6 (absorption).

^eWZ–GaN/sapphire (0001).

^fReference 27 (femtosecond four-wave mixing).

^gReference 13 (contactless electroreflectance).

^hReference 28 (spectroscopic ellipsometry).

ⁱReference 24 (contactless electroreflectance).

^jReference 29 (photoreflectance).

^kReference 30 (contactless electroreflectance).

IV. SUMMARY

In summary, a CER study on the Ga and N faces of a low defect concentration freestanding WZ–GaN sample has been performed in the temperature range between 20 and 300 K. The transition energies (A, B, and C excitons) and broadening parameters of the A and B excitonic transitions have been determined. The energy positions and separations of the transition energies reveal the existence of a small residual compressive in-plane strain. The temperature dependence of the A, B, and C exciton energies has been fit to both Varshni and Bose–Einstein-type expressions. At 20 K the smaller broadening parameter of the Ga face in relation to the N face corresponds to the lower defect density of the former surface. The broadening of the A and B excitons as a function of temperature indicates that the exciton–phonon interaction in GaN is very large.

ACKNOWLEDGMENTS

The work of the authors Y.S.H. and F.H.P. was supported by the New York State Science and Technology Foundation

through its Centers of Advanced Technology program. The work at VCU was funded by Grants from AFOSR (Dr. C. L. Witt and Dr. D. Johnson), ONR (Dr. C. E. C. Wood and Dr. Y. S. Park), and NSF (Dr. Varshney and Dr. Hess).

¹H. Morkoç, *Nitride Semiconductors and Devices* (Springer, Heidelberg, 1999).

²R. J. Molnar, R. Singh, and T. D. Moustakas, *Appl. Phys. Lett.* **66**, 268 (1995).

³M. A. Kahn, *Microwave J.* **36**, 67 (1993).

⁴S. C. Binari, K. Ikossi, J. A. Roussos, W. Kruppa, D. Park, H. B. Dietrich, D. D. Koleske, A. E. Wickenden, and R. L. Henry, *IEEE Trans. Electron Devices* **48**, 465 (2001).

⁵R. J. Molnar, W. Goetz, L. T. Romano, and N. M. Johnson, *J. Cryst. Growth* **178**, 147 (1997).

⁶A. J. Fischer, W. Shan, J. J. Song, Y. C. Chang, R. Horning, and B. Goldenberg, *Appl. Phys. Lett.* **71**, 1981 (1997).

⁷S. F. Chichibu, K. Torii, T. Deguchi, T. Sota, A. Setoguchi, H. Nakanishi, T. Azuhata, and S. Nakamura, *Appl. Phys. Lett.* **76**, 1576 (2000).

⁸J. F. Muth, J. H. Lee, I. K. Shmagin, R. M. Kolbas, H. C. Casey, Jr., B. P. Keller, U. K. Mishra, and S. P. DenBaars, *Appl. Phys. Lett.* **71**, 2572 (1997).

⁹K. Torii, T. Deguchi, T. Sota, K. Suzuki, S. Chichibu, and S. Nakamura, *Phys. Rev. B* **60**, 4723 (1999).

¹⁰R. Stepniowski, K. P. Korona, A. Wyszomolek, J. M. Baranowski, K. Pakula, M. Potemski, G. Martinez, I. Grzegory, and S. Porowski, *Phys. Rev. B* **56**, 15151 (1997).

¹¹W. Shan, B. D. Little, A. J. Fischer, J. J. Song, B. Goldenberg, W. G. Perry, M. D. Bremser, and R. F. Davis, *Phys. Rev. B* **54**, 16369 (1996).

¹²W. Shan, A. J. Fischer, S. J. Hwang, B. D. Little, R. J. Hauenstein, X. C. Xie, J. J. Song, D. S. Kim, B. Goldenberg, R. Horning, S. Krishnankutty, W. G. Perry, M. D. Bremser, and R. F. Davis, *J. Appl. Phys.* **83**, 455 (1998).

¹³C. F. Li, Y. S. Huang, L. Malikova, and F. H. Pollak, *Phys. Rev. B* **55**, 9251 (1997).

¹⁴Y. P. Varshni, *Physica (Amsterdam)* **34**, 49 (1967).

¹⁵P. Lantenschlager, M. Garriga, S. Logothetidis, and M. Cardona, *Phys. Rev. B* **34**, 2458 (1986).

¹⁶J. Lee, E. Koteles, and M. O. Vassell, *Phys. Rev. B* **33**, 5512 (1986).

¹⁷M. K. Kelly, R. P. Vaudo, V. M. Phanse, L. Gorgens, O. Ambacher, and M. Stulzmann, *Jpn. J. Appl. Phys., Part 2* **38**, L217 (1999).

¹⁸P. Visconti, K. M. Hones, M. A. Reshchikov, F. Yun, R. Cingolani, H. Morkoç, S. S. Park, and K. Y. Lee, *Appl. Phys. Lett.* **77**, 3743 (2000).

¹⁹F. H. Pollak and H. Shen, *Mater. Sci. Eng., R.* **10**, 275 (1999).

²⁰D. C. Reynolds, D. C. Look, W. Kim, O. Aktas, A. Botchkarev, A. Salvador, H. Morkoç, and D. N. Talwar, *J. Appl. Phys.* **80**, 594 (1996).

²¹See, for example, F. H. Pollak, in *Group III Nitride Semiconductor Compounds: Physics and Applications*, edited by B. Gil (Clarendon, Oxford, 1998), p. 158 and references therein.

²²S. F. Chichibu, A. Setoguchi, A. Uedono, K. Yoshimura, and M. Sumiya, *Appl. Phys. Lett.* **78**, 28 (2000).

²³R. J. Elliott, *Phys. Rev.* **108**, 1384 (1957).

²⁴W. Krystek, F. H. Pollak, Z. C. Feng, M. Schurman, and R. A. Stall, *Appl. Phys. Lett.* **72**, 1353 (1998).

²⁵L. Malikova, Y. S. Huang, F. H. Pollak, Z. C. Feng, M. Schurman, and R. A. Stall, *Solid State Commun.* **103**, 273 (1997).

²⁶P. Lantenschlager, M. Garriga, S. Logothetidis, and M. Cardona, *Phys. Rev. B* **35**, 9174 (1987).

²⁷A. J. Fischer, W. Shan, G. H. Park, J. J. Song, D. S. Kim, D. S. Yee, R. Horning, and B. Goldenberg, *Phys. Rev. B* **56**, 1077 (1997).

²⁸J. Petalas, S. Logothetidis, S. Bouladakis, M. Alouani, and J. M. Wills, *Phys. Rev. B* **52**, 8082 (1995).

²⁹H. Qiang, F. H. Pollak, C. M. Sotomayor Torres, W. Leitch, A. H. Kean, M. Stroschio, G. J. Iafrate, and K. W. Kim, *Appl. Phys. Lett.* **61**, 1411 (1992).

³⁰L. Malikova, W. Krystek, F. H. Pollak, N. Dai, A. Cavus, and M. C. Tamargo, *Phys. Rev. B* **54**, 1819 (1996).